Seismic interferometry technique for characterization of loose soil layers

Seda Gokyer Erbis[1*], *William Allen* Marr[1], *Thomas* Bardainne[2], *Renaud* Tarnus[2]

[1]*Geocomp, Inc.,125 Nagog Park Acton MA 01720, USA*
[2]*Sercel, Infrastructure Monitoring, 27 Avenue Carnot Massy, France*
[*]*seda.gokyererbis@geocomp.com*

ABSTRACT

Surface wave tomography is a feasible method to provide complementary data to better understand the continuity of soil strata. It may also be used to determine best locations for invasive testing. Surface wave tomography methods are frequently used to delineate soil-rock interface and determine average shear wave velocity for seismic site class determination. Delineation within the soils layers where the change in seismic velocity within the soil layers are relatively small requires higher resolution data collection and enhanced processing methods than those used historically in surface wave tomography.
This study uses a patented imaging and monitoring system based on the passive seismic interferometry technique augmented by active seismic sources at known locations. A dense nodal array of MEMs accelerometers were deployed at a site where known saturated loose materials exist. This paper presents shear wave velocity (V_s) data deduced from surface wave measurements where various, compression wave velocity (V_p) to V_s ratios were considered, especially showing the effect of V_p/V_s ratio, on the V_s data. This ratio which was traditionally assumed can have a significant effect on the inferred V_s. This paper also presents the comparison of deduced V_s data to measured V_s data by seismic cone penetration test and makes some recommendations for how to improve the methods to determine shear wave velocity in soft/loose soils.

Keywords: ambient seismic noise; interferometry; surface waves; soft soils; accelerometers.

1. Introduction

Characterizing near surface soils, rock and groundwater conditions is one of most, if not the most important step in geotechnical engineering to achieve successful design of infrastructure and minimize the risks associated with the uncertainty within the subsurface. The state of practice for geotechnical investigations typically involves soil borings and standard penetration and cone penetration testing to characterize the subsurface. However, the standard practice for ground exploration still relies on field borings or in-situ tests at discrete locations and requires assumptions of the subsurface conditions between discrete exploration locations. These assumptions may not lead to reasonable estimates of the strata especially when saturated loose/soft soils exist within the subsurface which are critical for stability of infrastructure such as embankments, tailings dams, etc... Current practice does not generally capture the spatial and temporal changes within the subsurface.

Geophysical imaging techniques, such as Multichannel Analysis of Surface Waves (MASW) or seismic interferometry, can provide a continuous 2D or 3D profile of subgrade properties such as shear wave velocity with depth along an investigated line. These methods are nondestructive, noninvasive, and relatively quick.

This paper presents a study where the proposed method is an approach derived from seismic interferometric methods augmented with known seismic source points.

To evaluate the feasibility of the proposed method, this study conducted a case study at a site with known subsurface information such as seismic cone penetration test, where saturated, soft materials exist.

2. Project Description

Selected project site is a coal combustion residual (CCR) facility which retains saturated and loose CCR materials as well as underlying soft foundation soils.

Fig. 1 shows (a) the project site, (b) and (c) critical cross sections at the site. The extent of these critical layers are a great concern in regards to the stability of the facility. The seismic interferometry survey was designed as line arrays along the two critical cross sections at the facility where existing geotechnical investigation data presented potential saturated and loose soil layers. The sensors used in these line arrays for data acquisition are self-powered accelerometers called WiNG^{NT} sensors containing QuietSeis^{TM} micro electro mechanical system (MEMs) accelerometers, referred as 'nodes' in this paper.

Line 1 (L1) was 209 ft long included 105 nodes with approximately 2 ft spacing between nodes. Line 2 (L2) was 331 ft long included 166 nodes similarly with 2 ft spacing.

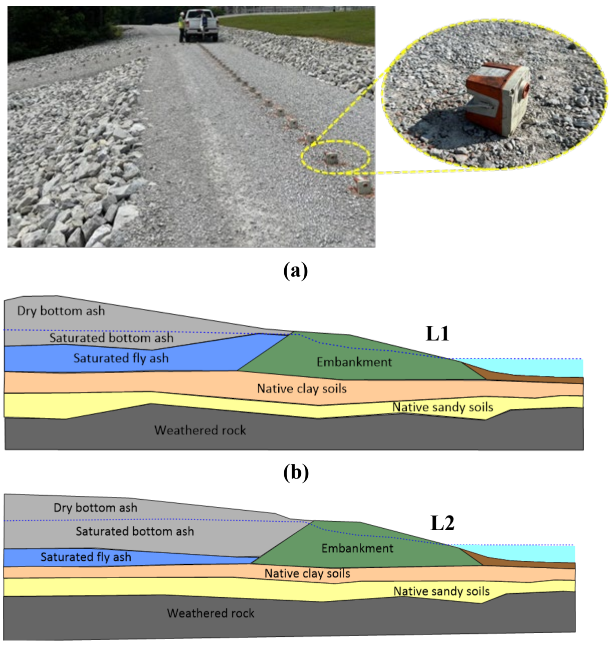

Figure 1. (a) Photograph from the site during seismic data collection, (b) Cross section for L1 and (c) Cross section for L2 from the site

3. Methodology

3.1. Interferometry

The presented seismic interferometry is hybrid solution is a high-resolution imaging technique which uses passive interferometry augmented with sparse stimulation using seismic sources with known locations. This hybrid solution benefits from the higher energetic potential of active sources, while greatly reducing their amount, making the acquisition process easier and faster. This process maintains high spatial resolution over the integrality of the survey with the use of interferometry. The resolution of the collected data greatly improves with the quality of the noise source. These sources include trains, propelled energy generators, sledgehammers, or pure ambient noise (Bardainne 2022) (Bardainne et al. 2023).

The first step of the interferometry methodology is to cross correlate source-receiver pairs by passive seismic interferometry. Ambient seismic noise can be used for underground imaging (Campillo and Paul 2003). The cross-correlation of a signal recorded by a pair of receivers A and B can create a virtual source-receiver pair respectively from A to B. Surface waves are particularly suitable for interferometry. The efficiency of seismic interferometry is substantially influenced by the alignment between the source of the seismic waves and the receiver.

Fig. 2 (a) shows the sensor diagram together with the noise source, example source-receiver pair of A and B. Interferometry cross-correlates two signals recorded on couples of sensors, revealing similarities that will be retained as a delay in propagation time, here for surface waves. Cross-correlating records from a large combination of sensors allows reconstructing an analyzable "virtual" waves packet encompassing the whole linear profile of sensors as shown in Fig. 2 (a).

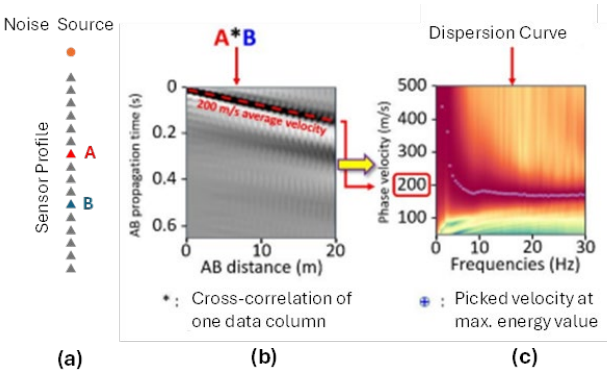

Figure 2. (a) seismic interferometry sensor profile with noise source, (b) cross correlated surface wave packet from a receiver pair, (c) example dispersion curve

Subsequent to matching source-receiver pair, the next step is to sum the cross-correlated signals from all receiver pairs to enhance the signal-noise ratio. The result of each cross-correlation depends on the intrinsic ground propagation velocity between a given pair of receivers. Fig. 2 (b) shows an example cross correlated surface wave packet from a receiver pair. Cross-correlation is performed on the largest valid combination of sensor couples that can be obtained from the network, building a so-called correlation map.

The next post-processing step is the computation of the dispersion diagrams, example shown in Fig. 2 (c). This step involves an adaptation of the Matched Field Processing (MFP) methodology (Jensen et al. 2003). MFP considers the known positions of an array of sensors to reconstruct the highly sensitive surface wave phase velocity as a function of frequency (i.e. dispersion curve). These processes involve the selection of groups of contiguous virtual traces along a selected length equivalent to a probing "antenna" or "patch" where MFP processing is applied to each patch.

The next step is the depth inversion of phase velocity picked from the dispersion curve. The wave packet is composed of many single wavelength waves. If the ground shows density or stiffness variations, the packet will "disperse", as the propagation velocity v, each frequency f and its associated wavelength L are interdependent through the relationship $L = v / f$ shown in Fig. 2 (c). This separation of the waves in depth and velocity allows to estimate shear wave velocity with depth. Each frequency sounding's surface location is then positioned at its associated selection antenna (or patch) geometric center.

The final step of the processing is to combine multiple one dimensional inversions which allows for producing a quasi-continuous profile of shear wave velocity data, similar to the one presented in the Fig. 3.

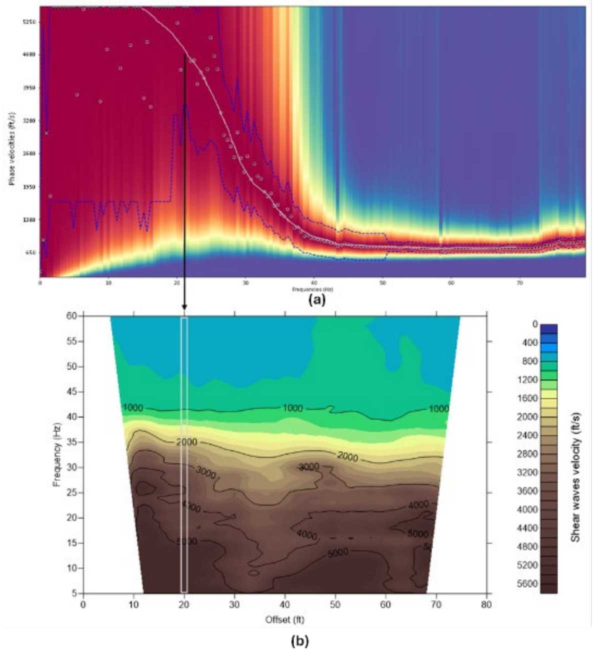

Figure 3. (a) Shear wave velocity inversion from dispersion curve, (b) quasi-continuous profile of inverted shear wave velocity data

4. Results and Findings

4.1. Site-specific with prior site data

There were geotechnical investigation data available for comparison which includes borings with standard penetration tests, seismic cone penetration test soundings.

Existing geotechnical data showed that the shear wave velocity ranges observed for the subsurface layers at the site is as follows: (1) embankment material between 700 to 1650 ft/s, (2) CCR materials above the phreatic surface between 750 to 1000 ft/s, (3) saturated CCR materials between 250 to 650 ft/s, (4) natural clay soils between 550 to 750 ft/s, (5) natural sandy soils between 600 to 1050 ft/s, (6) fractured shale rock between 800 to 1800 ft/s. Both cross sections (L1 and L2) comprised of similar soil layers with some differences in their thicknesses.

The phreatic surface at this site is approximately 5 to 10 ft below the ground surface. A rule of thumb value for the ratio between compression wave velocity, V_p and the shear wave veloctity, V_s is approximately 2.5 in surface wave analysis. However when soil layers are saturated such as the saturated loose CCR layer below the phreatic surface at this site, this ratio can change substantially because V_p increases to approximately 5000 ft/s and V_s is low if the material is loose. This ratio which was traditionally assumed can have a significant effect on the inferred V_s also shown by others (Qin et al. 2020)

Prior data available from similar sites was used to estimate site specific V_p/V_s ratio for this project site to improve the shear wave velocity estimates from the surface wave measurements as shown in Table 1.

Table 1. Site specific priori data

Layer	V_p/V_s Values
Soil Layers above phreatic surface	2.3
Soil Layers below phreatic surface	6.8
Rock layer	2.3

4.2. Seismic interferometry results

For Line 1 (L1), shear wave velocity inversion was conducted using the prior V_p/V_s information by assuming three subzones with different V_p/V_s as shown in Table 1. Within the sublayers corresponding V_p/V_s value kept constant. In this study, using the results from L1, we explored the feasibility of multiple subzones with different V_p/V_s compared to assuming a single V_p/V_s value that represents the whole profile. For Line 2 (L2) shear wave velocity inversion was conducted only using fixed V_p/V_s ratios of 2.3 and 6.8.

Fig. 4 presents the shear wave velocity results for L1 as a contour map where three different cases of V_p/V_s. Fig. 4 (a) presents results where V_p/V_s=2.3 for the whole cross section, (b) where V_p/V_s=6.8 for the whole cross section, and (c) where the V_p/V_s was varied between the three sublayers.

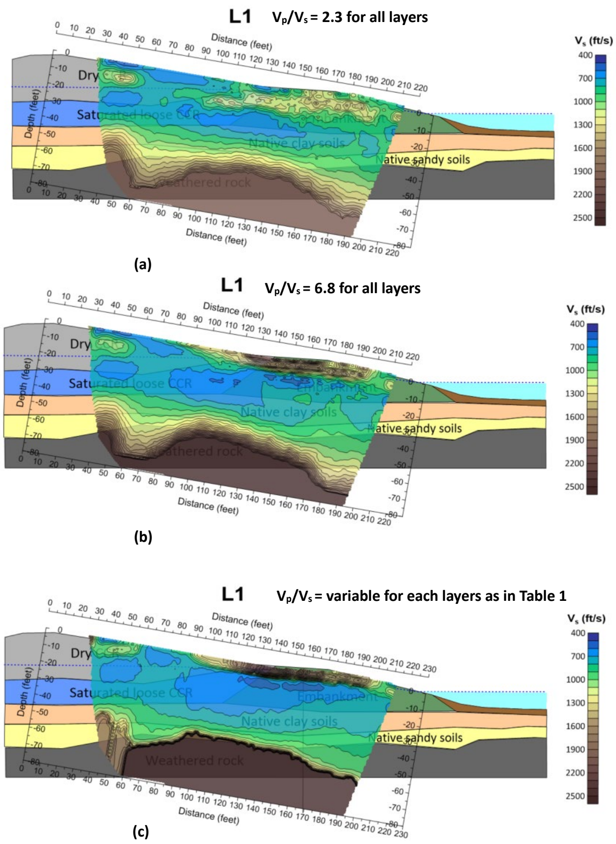

Figure 4. Passive seismic shear wave velocity results for Line 1 (a) V_p/V_s=2.3, (b) V_p/V_s=6.8, (c) variable V_p/V_s

The shear wave velocity results determined considering higher V_p/V_s ratio were more successful in detecting the expected contrast between the loose CCR material and other soil layers such as the embankment and natural soils.

Fig. 5 presents the same set of results digitized for line chart at station 155 ft which is close to the approximate location of in-situ tests. In Fig. 5, seismic interferometry results are compared with existing geotechnical field data available i.e. measured V_s data from seismic cone penetration test (sCPT) data, correlated V_s data from cone penetration test (CPT) and standard penetration test (SPT). Based on the prior data, embankment layer within the top 25 ft is not a homogeneous layer with shear wave velocity range between 700 to 1650 ft/s and as shown in Fig.5 the data suggests that the top 10 ft of the embankment layer is denser than the bottom 15 ft of the embankment layer.

Both the measured downhole sCPT data and correlated CPT data indicated there is a denser layer within top 15 ft below the ground surface corresponding to the top portion of embankment. The measured sCPTu data is higher than the correlated CPT data especially for the embankment layer. Correlations from CPT tip and sleeve resistance are typically empirically correlated to data sets from naturally deposited soils. The performance of correlations for unique materials such as CCR or compacted deposits such as embankments is expected to differ. Consistent with this expectation, measured and correlated field data agreed relatively well for the natural soil layers below the embankment, at the depths lower than 25 ft below the ground surfac whereas the agreement was not as good for the embankment layer between 0 to 25 ft below ground surface.

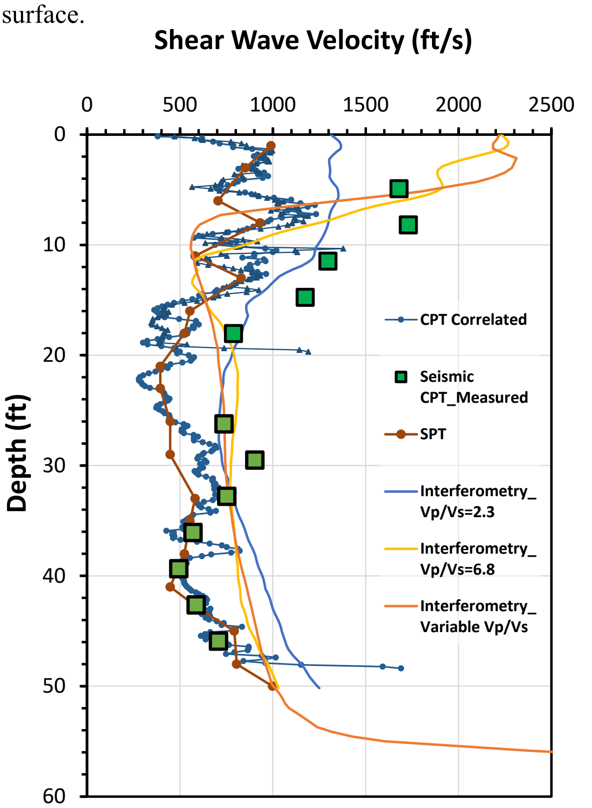

Figure 5. Digitized passive seismic shear wave velocity results at station 155 ft compared with existing geotechnical data

Seismic interferometry results from different V_p/V_s values presented in Fig. 5 showed that the shear wave velocity results using rule of thumb value of V_p/V_s=2.3 did not perform as good as the other two cases with V_p/V_s=6.8 and variable V_p/V_s. Seismic interferometry results determined using V_p/V_s=6.8 and variable V_p/V_s were able to capture the contract between the embankment layer and below natural soils. For depths lower than 35 ft or larger below ground surface, the agreement between the seismic interferometry results and measured and correlated shear wave velocity data was not as good. This can be attributed to the limitation in resolution of results below 35 ft or larger below the ground surface.

Fig. 6 presents the shear wave velocity results for L2 as a contour map (a) where V_p/V_s=2.3 for the whole cross section, and (b) where V_p/V_s=6.8 for the whole cross section. L2 results are in general similar to L1 results that the contrast between the loose CCR layers and embankment layers are more distinct in the results computed with V_p/V_s=6.8. However the effect of V_p/V_s ratio was not as prominent in L2 then L1, which could be attributed that the site-specific V_p/V_s ratio for this cross section might not be well represented by value 6.8.

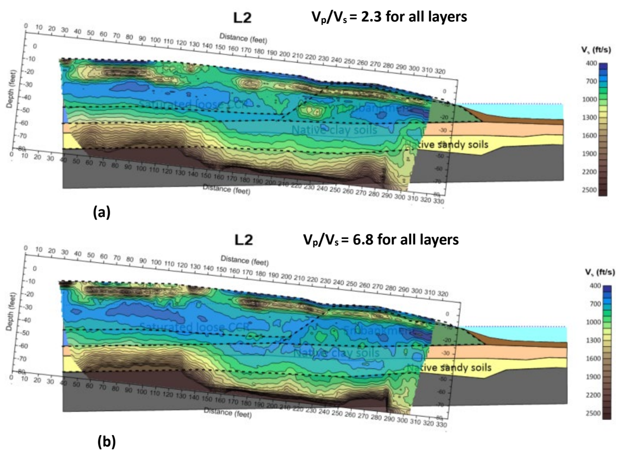

Figure 6. Passive seismic shear wave velocity results for Line 2 (a) V_p/V_s=2.3, (b) V_p/V_s=6.8, (c) variable V_p/V_s

Fig. 7 presents the same set of results digitized for line chart at station 260 ft compared with only correlated V_s data from cone penetration test. Unfortunately there were not any measured downhole shear wave velocity value available for this location. The seismic interferometry results are only compared to the correlated shear wave velocity data from CPT. Correlated CPT Vs data shows that top 20 ft is slightly denser than the below. This layer corresponds to the top denser section within the embankment layer. Seismic interferometry results using both V_p/V_s=2.3 and V_p/V_s=6.8 captured denser and more compacted top layer within 0 to 10 ft similar to L1 along the other cross section where CPT correlated data did not capture. Correlated shear wave velocity data from CPT suggested bottom 20 ft deep loose natural soils below the embankment.

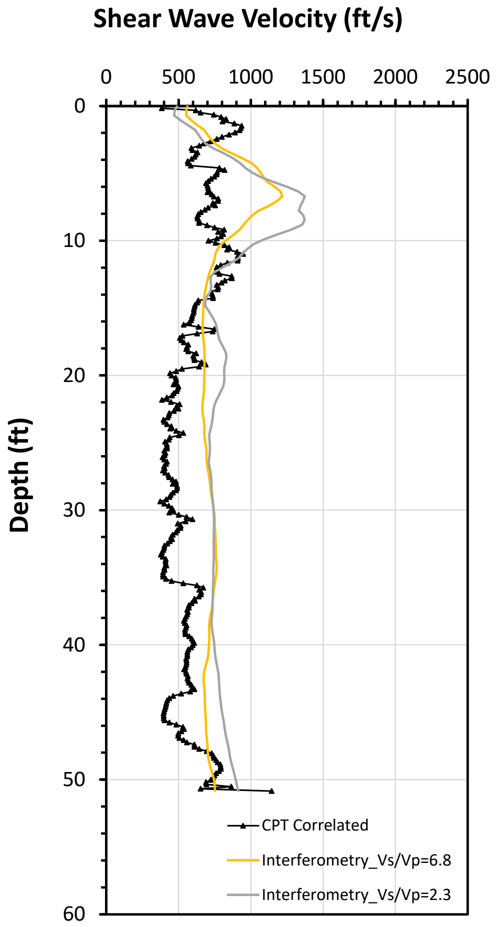

Figure 7. Digitized passive seismic shear wave velocity results at station 155 ft compared with existing geotechnical data

4.3. Discussion

When the seismic interferometry results are analyzed together with prior data, the effect of V_p/V_s on the shear wave velocity estimated from surface wave analysis is apparent. If the project goal is to characterize a site with loose or soft soils layers, site-specific V_p/V_s is a key input for the surface wave inversion.

Both cases with fixed V_p/V_s=6.8 and variable V_p/V_s as opposed to V_p/V_s=2.3 represented the expected delineation of the subsurface layers and detected a better contrast between the compacted near surface layers and deeper looser or softer natural soils and moreover detected the lower V_s values for the saturated loose CCR layers more accurately. However there is marginal difference between the velocity results using V_p/V_s=6.8 and variable V_p/V_s, given both cross sections were primarily comprised of saturated soft or loose materials. Therefore, varying the V_p/V_s ratio within the same cross section was found to be not as feasible as finding the most representative but a single value of V_p/V_s ratio for the cross section. For profiles at this site, the dominant layers were saturated and loose soil layers and the seismic interferometry results from fixed V_p/V_s=6.8 was representative. However, this study still observed differences in velocity results measured with sCPTu data and interferometry results with site-specific V_p/V_s , it should be noted that the sCPTu data at this project site was limited.

All seismic interferometry results for L1 and L2 detected the rock layer as soft rock with Vs values ranging 750 ft/s to 1750 ft/s which is very consisted with the prior data collected at the site for fractured shale rock which is between 800 to 1800 ft/s.

5. Conclusion

Seismic interferometry results can capture the soft deposited CCR layers well especially if the ash layer is surrounded by layers such as embankment with higher V_s. When compared with available in-situ geotechnical data, V_s results from seismic interferometry has a relatively good agreement with measured V_s values.

The V_s results improve with prior data from the site such as knowledge of phreatic surface, existence of soft soils by applying the prior information more applicable instead of a rule of thumb value such as site-specific V_p/V_s.

The further development in processing of seismic interferometry is in progress for improving the data resolution by aiming to estimate the site-specific V_p/V_s from measured surface wave analysis employing seismic refraction technique. More accurate estimation of site-specific V_p/V_s will enable more accurate estimation of V_s from surface wave measurements.

Acknowledgements

The authors are grateful for the financial support provided by our anonymous client. The authors are also grateful for having the prior data available at this site to be used for this study.

References

Bardainne, T. "Monitoring the physical condition of a longitudinal element". France Patent FR3114886B1. 11 11., 2022

Bardainne, T., Tarnus, R., Vivin, L., Cai, C., Rebert, T., Allemand, T., Toubiana, H. "Stimulated Noise and Surface Wave Interferometry Processing for Hybrid Seismic Imaging", In: 29th European Meeting of Environmental and Engineering Geophysics, Edinburgh, United Kingdom, 2023, pp.1-5. https://doi.org/10.3997/2214-4609.202320206

Campillo, M. & Paul, A. "Long-range correlations in the diffuse seismic coda", Science, 299(5606), 547. 18, 87, 2003.

Jensen, F. B., Kuperman, W. A., Porter, M. B., and Schmidt, H. "Computational Ocean Acoustics", 2nd ed. New York, 2011, Springer-Verlag. https://doi.org/10.1007/978-1-4419-8678-8

Qin L., Ben-Zion, Y., Bonilla F. L., Steidl, J.H., "Imaging and Monitoring Temporal Changes of Shallow Seismic Velocities at the Garner Valley Near Anza, California, Following the M7.2 2010 El Mayor-Cucapah Earthquake", Journal of Geophysical Research: Solid Earth, 125, 2020.